Effects of Lithiation on Melting Temperature (T_m) and Diffusion Kinetics of Spinel $Li_{4+x}Mn_5O_{12}$ ($0 \leq x \leq 3$).

R.S. Ledwaba, M.G. Matshaba and P.E. Ngoepe

Materials Modelling Centre, University of Limpopo, Private Bag X 1106, Sovenga,0727, South Africa

Email: raesibe.ledwaba@ul.ac.za

Abstract: The investigation of high temperature effects on lithium-rich spinel $Li_{4+x}Mn_5O_{12}$ cathode material was carried out by employing molecular dynamics simulations in the range 300-3000K, under the NVE ensemble. Energy graphs for all systems showed no obvious phase transition from room temperature up to the melting points of each system, where the latter is directly proportional to lithium concentration i.e. the latent heats of fusion on each total energy graph increased with an increase in lithium concentration. The anomalous changes in diffusion of Li above the melting temperatures (exponential increase in diffusion coefficients) may be related to dynamic distortion of the oxygen tetrahedron surrounding the Li atom, which is necessary to make it diffuse. However, a reduction in lithium ion diffusion with increasing lithium concentration observed in $Li_{4+x}Mn_5O_{12}$ is attributable to full occupancy of 16c sites by lithiums closer to $Li_7Mn_5O_{12}$, thus compelling any further inserted lithiums to occupy 8a sites which are energetically unfavourable.

1. Introduction

The enhanced electrochemical performance of spinel Li-Mn-O cathode materials, driven by the three-dimensional framework, has fuelled an enormous interest for their utilisation in portable electronics, electric vehicles and renewable energy storage [1, 2]. These properties have triggered more curiosity for persuasion of further studies on the diffusion kinetics, structural and dynamic properties of spinel $Li_{x+1}Mn_{2-x}O_4$ [3, 4, 5]. One such study was the ab initio molecular-dynamics calculations, based on the structural and diffusive properties of spinel. The study indicated that only the Li ions diffuse, as compared to diffusion of both Mn and Li ions identified by Ouyang et al [4]. In terms of host capability, it was indicated that lithiating $Li_{4+x}Mn_5O_{12}$ with up to 3Li ions per formula unit to form $Li_7Mn_5O_{12}$, could provide a high capacitance and demonstrated that the charge transfer resistance for the $Li_4Mn_5O_{12}$ electrode is small i.e. the electrode material had good capacitive behaviour [5]. Furthermore, when the behaviour of lithiums in the spinel structure was monitored, there was an occurrence of self-diffusion of Li atoms as a result of periodical distribution of Mn valences. Although this was predicted to be a result of distortion of LiO_4 tetrahedral faces [3], Ishizawa et al pointed out that much was yet to be understood about the nature of Li diffusion in the cathodes under development despite the extensive studies that have been carried out on the positive electrode materials [6]. In the current study, we carry out the high temperature molecular dynamic simulations on lithiated spinel lithium manganese oxides ($Li_{4+x}Mn_5O_{12}$ where ($1 \leq x \leq 3$)), driven by the significant interest of the material's application as a cathode in lithium ion batteries. These simulations will add valuable

insights towards the understanding of high temperature behaviour i.e. various melting points, lithium ion diffusion and structural transformations at elevated temperatures, as well as other aspects that may contribute towards the performance of a battery material.

2. Computational Methods

2.1. Generation of Systems

Lithium atoms were inserted into the 16c vacant positions (Wyckoff sites) of the $Li_4Mn_5O_{12}$ bulk structure in order to generate lithium intercalated models that will be represented by $Li_{4+x}Mn_5O_{12}$ ($1 \leq x \leq 3$). The METADISE code [7] was utilised for generation of DL_POLY input files required for simulations and generation of 6x6x6 supercell systems from conventional unit cells with (a) 56-$Li_4Mn_5O_{12}$, (b) 58-$Li_5Mn_5O_{12}$, (c) 61-$Li_6Mn_5O_{12}$ and (d) 64 atoms-$Li_7Mn_5O_{12}$.

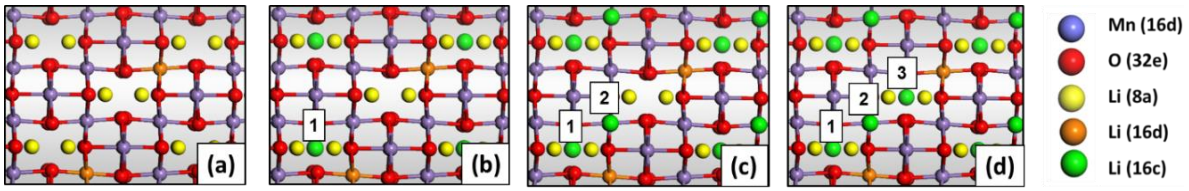

Figure 1: Conventional unit cells of spinels (a) $Li_4Mn_5O_{12}$ with 56 atoms (b) $Li_5Mn_5O_{12}$ with 58 atoms (c) $Li_6Mn_5O_{12}$ with 61 atoms and (d) $Li_7Mn_5O_{12}$ with 64 atoms. Colour notation: Mn= 16d (purple); O= 32e, Li= 8a (yellow); Li =16d (orange); Li = 16c (green). Numerical labels (1, 2, 3) represent the 3 16c vacant sites in the conventional unit cell.

2.2 .The Potential Model

Interatomic potentials used in this study were generated and reported previously for the Born model of the ionic solid, in which the Mn^{4+}, Mn^{3+}, Li^+ and O^{2-} ions interact via long-range Coulombic interactions and short-range parameterized interactions [8] used in our previous work during the molecular dynamic simulations of pure spinel $LiMn_2O_4$ [9].

3. Results and discussion

3.1. X-ray Diffraction Patterns

Figure 1 (a) and (b) show the XRD patterns of the spinel $Li_4Mn_5O_{12}$ obtained from experimental work and calculated in this work, respectively. The characteristic peaks indexed in figure 1(a) represent indices for a face centred cubic structure [5] and are comparable to peaks observed in (b) for the model of $Li_4Mn_5O_{12}$ used in this work. Figure 1. (c), depicts XRD of lithiated spinel $Li_7Mn_5O_{12}$, with clear peak shift in between $2\Theta = 36$ and 38^0 due to the insertion of lithiums in 16c sites. Each of the XRDs have an image (top right corner) that indicates atomic arrangements before and after lithiation.

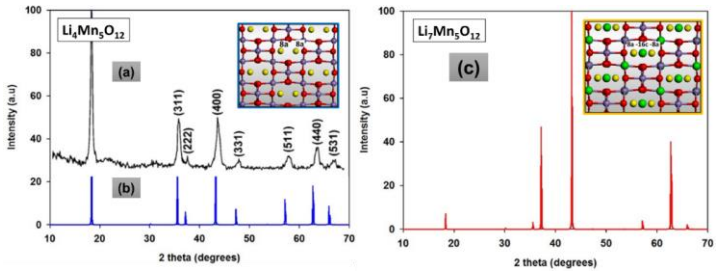

Figure 2: XRD patterns and images of atomic arrangements for spinel $Li_4Mn_5O_{12}$ (a) experimentally [5] and (b) model (56 atoms), and (c) $Li_7Mn_5O_{12}$ (64 atoms) where yellow spheres represent Li in 8a sites and green spheres represent Li in 16c sites.

3.2. Pair Distribution Functions and Total Energy graphs

The radial distribution function plots assist with the identification of crystalline to amorphous phase transitions for spinel $Li_{4+x}Mn_5O_{12}$ ($1 \leq x \leq 3$), when subjected to high temperature. Each graph consists of an insert to clearly demonstrate changes on the plots, as temperature is increased. In (a), the plots between 300K and 1500K show a constant decrease in peak height, followed by broader peaks between 1700 K and 3000K. This effect of temperature is illustrated clearer on the insert enclosed in a blue box, depicting merger of peaks as temperature is increased i.e. 2nd (A=~3.5 Å) and 3rd (B=~5.0 Å) peak merge into a single flatter peak (C= ~4.3 Å). The rdfs suggest that melting temperature of spinel $Li_5Mn_5O_{12}$ is approximately 1700 K and this is good accord with total energy graph in (b), which a depicts linearly increasing graph until reaching latent heat of fusion (transitions between A and B), then becoming linear again after the change in phase. Similar behaviour is observed in (c), where rdfs for $Li_6Mn_5O_{12}$, above 2000K, depict merger between peaks A and B to form C suggesting transformation to an amorphous phase and are supported by the total energy graph in (d), clearly depicting a jump between A and B suggesting T_m around 2300K. Lastly, rdfs for $Li_7Mn_5O_{12}$ (e) shows broader peaks above 2500K and the merger of peak A and B in the insert enclosed in a green box, where peak C occurs at 2500K and 3000K as a property of amorphous system. The total energy versus temperature for (f) $Li_7Mn_5O_{12}$ adheres to a linear trend until the material reaches its melting point at 2 700K. The trends observed in these graphs suggest that an increase in lithium concentration encourages higher melting temperature.

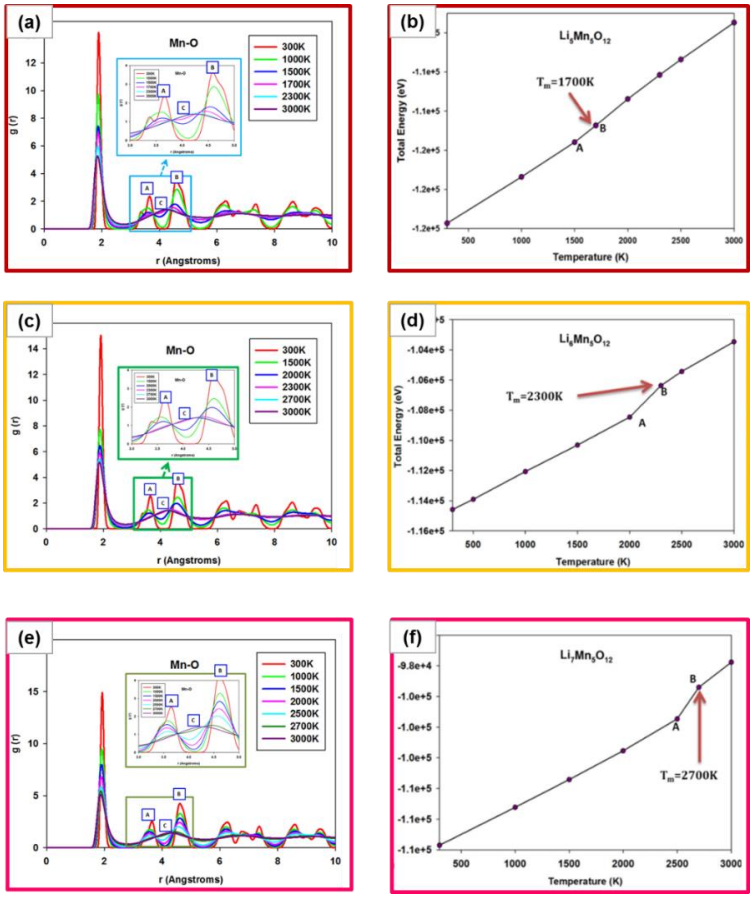

Figure 3: Radial distribution functions (Mn-O bonds) and total energy graphs for spinels: (a, b) $Li_5Mn_5O_{12}$, (c, d) $Li_6Mn_5O_{12}$ and (e, f) $Li_7Mn_5O_{12}$ in the temperature range.

3.3. Diffusion Coefficients

Figure 3 illustrates the diffusion coefficient graphs for (a) $Li_5Mn_5O_{12}$, (b) $Li_6Mn_5O_{12}$ and (c) $Li_7Mn_5O_{12}$ plotted as a function of temperature. The graph for spinel $Li_5Mn_5O_{12}$ (a), illustrates a slight mobility of lithium ions around 300K, which increases minimally until an exponential increase between 1500K-3000K. The increase at 1500K is coupled with mobility of the manganese and oxygen ions, and occurs in the range of phase transition observed on both the total energy and rdf graphs. In (b), lithium cations also show slight mobility above 500 K, then the oxygen and manganese only move around 2000K, just before the melting point. This trend is also observed for spinel $Li_7Mn_5O_{12}$, where the lithium cations show mobility above 500 K and the other ions only move at temperature above melting point. We can predict that the oxygen and manganese ions only show mobility after the melting point has been reached, in each system. This decrease in lithium ion mobility with an increase in lithium concentration may be associated with the very poor lithium-ion conductivity of $Li_7Mn_5O_{12}$ comparable to $Li_7Ti_5O_{12}$ previously reported to be due to full occupancy of lithiums in the 16c sites thus resulting occupancy of Li in 8a sites which are energetically unfavourable [10].

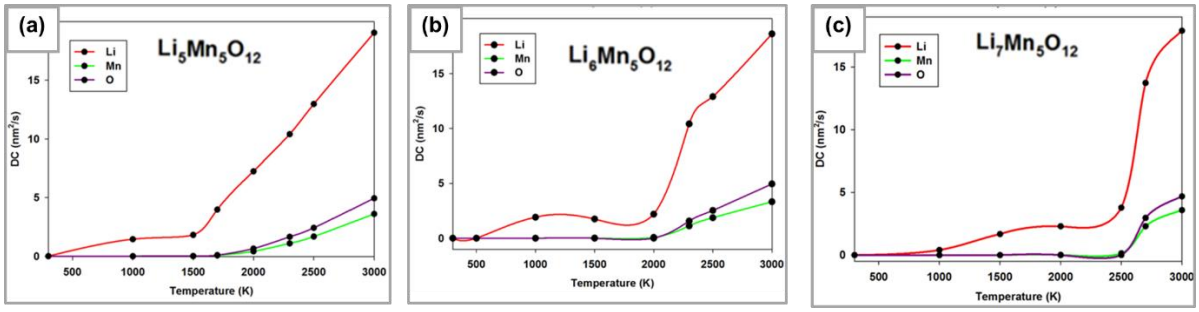

Figure 4: Diffusion coefficients for spinel: (a) $Li_5Mn_5O_{12}$, (b) $Li_6Mn_5O_{12}$ and (c) $Li_7Mn_5O_{12}$.

4. Discussion

The rdf graphs illustrated an increase in melting temperature with an increase in lithium concentration. These were supported by the total energy graphs, which also showed no obvious phase transitions from room temperature up to the melting points of each system. The diffusion observed for $Li_{4+x}Mn_5O_{12}$ at high temperatures (>500 K) is mainly ascribed to lithium transport between vacant 16c sites through tetrahedral 8a sites as suggested by Tateishi et al [3] and adopt a trend similar to that of the spinel $Li_{4+x}Ti_5O_{12}$, with 3D tunnel framework [11]. Generally Li diffusion in $Li_{4+x}Mn_5O_{12}$ commences earlier than those of other ions, however, the anomalous changes in diffusion of Li above the melting temperatures are noted at higher temperatures may be related to dynamic distortion of the oxygen tetrahendron surrounding the Li atom, which is necessary to make it diffuse. These observations imply that an increase in lithium ion concentration results in a lower diffusion coefficient for systems observed at the same temperature i.e. higher lithium concentration requires larger activation energy. An interesting trend was observed for diffusion of lithiated $Li_{4+x}Mn_5O_{12}$ where systems with more lithiums had less lithium ion diffusion similar to $Li_{4+x}Ti_5O_{12}$ systems, where the activation energy for lithium hopping between the 16d and 16c sites was a linear function of the lithium content with activation energies [11]. These observations implied that an increase in lithium ion concentration resulted in a lower diffusion coefficient for systems observed at the same temperature i.e. higher lithium concentration requires larger activation energy. Although the Li diffusion of the spinel manganese oxides at room temperature is desirable for use in battery materials the current study has shed valuable insights on structural and transport properties at high temperatures.

5. Conclusion

In the current study, we carried out molecular dynamic simulations on the supercell systems of spinel $Li_{4+x}Mn_5O_{12}$ ($0 \leq x \leq 3$), lithiated up to $Li_7Mn_5O_{12}$. The study predicted increase in melting

temperature with an increase in lithium concentration and dependence of diffusion rate on LiO_4 distortion acquired during the melting temperature as well as hindrance of diffusion rate at high concentrations by full occupancy of 16c sites.

Acknowledgements
We acknowledge support of the South African Research Chair Initiative of the Department of Science and Technology and the National Research Foundation in Pretoria and the Centre for High Performance Computing in Cape Town.

References

[1] Manthiram A 2011 *J. phys. chem. lett.* **2** 176
[2] Long B R, Croy J R, Park J S, Wen J, Miller D J and Thackeray M M 2014 *J. electrochem. soc.* **161** A2160
[3] Tateishi D, Boulay D and Ishizawa N 2004 *J. ceram. soc. jpn.* **112** S658
[4] Ouyang C Y, Shi S Q, Wang Z X and Li H, 2004 *Europhys. lett.* **67** 28
[5] Hao Y J, Lai Q Y, Xu X Y and Wang L 2011 *Mater. chem. phys.* **126** 432
[6] Ishizawa N and Tateishi K 2009 *J. ceram. soc. jpn.* **117** 6
[7] Watson G W, Kelsey E T, De Leeuw N H, Harris D J and Parker S C, 1996 *J. chem. soc.* **92** 433
[8] Maphanga R R, Sayle T X T, Ngoepe P E and Sayle D C 2011 *Phys. chem. chem. phys.* **13** 1307
[9] Ledwaba R S, Matshaba M G and Ngoepe P E 2015 *IOP conf. ser. mater. sci. eng* **80** 012024
[10] Yao X L, Xiea S, Nian H Q and Chena C H 2008 *J. alloys compd.* **465** 375
[11] Vijayakumar M, Kerisit S, Rosso K M, Burton S D and Sears J A, Yang Z, Graff G L, Liu J and Hu J 2011 *J. power sources* **196** 2211